Available online at www.sciencedirect.com
SCIENCE DIRECT®
Mechanics of Materials 38 (2006) 160–170
MECHANICS OF MATERIALS
www.elsevier.com/locate/mechmat

Strain-rate effect and micro-structural optimization of cellular metals

J.L. Yu *, J.R. Li, S.S. Hu

CAS Key Laboratory of Mechanical Behavior and Design of Materials, University of Science and Technology of China, Hefei 230026, China

Abstract

An overview is given of the researches at USTC on mechanical properties of cellular metals including aluminum honeycombs and foams. The strain-rate effect and micro-structural optimization of cellular metals are reported. The in-plane quasi-static and dynamic behavior of circular-cell aluminum alloy honeycombs is investigated experimentally. The influence of impact velocity on the localized deformation mode and the plateau stress are found. The strain-rate effect and the cell-size effect on the crushing stress of both open-cell and closed-cell aluminum foams are investigated by an improved Split Hopkinson Pressure Bar method. The results reveal that the structural heterogeneity and irregularity have influence on the strain-rate sensitivity of cellular metals. The effect of multi-size cell mix and silicate-rubber filler on the mechanical properties of open-cell aluminum foams is studied. The results show that it is a possible way to improve the mechanical properties of open-cell foams by mixing multi-size cells and by filling silicate-rubber.

Keywords: Mechanical property; SHPB; Aluminum; Foams; Honeycombs

1. Introduction

During the last two decades metallic foams have been developed and are growing in use as new engineering materials. These ultra-light metal materials possess unique mechanical properties, such as high specific rigidity and high impact energy absorption at low weight, equal properties in all directions giving tolerance to varying direction of loading, stable deformation mode and adaptation to loading condition during deformation, etc. Potential applications include energy absorbers in the automotive industry and other equipment for transportation, packaging (protection from shock for heavy components that are sensitive to impact), core material in sandwich structures with special requirements, and core material in hollow structures to prevent buckling.

* Corresponding author. Tel.: +86 551 360 3793; fax: +86 551 360 6459.
E-mail address: jlyu@ustc.edu.cn (J.L. Yu).

0167-6636/$ - see front matter © 2005 Elsevier Ltd. All rights reserved.
doi:10.1016/j.mechmat.2005.05.018

1.1. Quasi-static mechanical behavior

When a block of foam is compressed, the stress–strain curve shows three regions, as shown in Fig. 1. At low strains, the foam deforms in a linear-elastic way, then a plateau of deformation at almost constant stress occurs, and finally there is a region of densification. The extent of each region depends on the relative density ρ/ρ_s. Elastic foams, plastic foams, and even brittle foams all have generalized three-part stress–strain curves like this, though the mechanism is different in each case.

The Young's modulus and compressive strength of metallic foams have been measured by a number of researchers (Prakash et al., 1995; Beals and Thompson, 1997; Sugimura et al., 1997; Andrews et al., 1999). However, most commercially available cellular metals, unlike some of their polymer counterparts, do not achieve the properties predicted by theoretical models according to the properties of the cell wall material and the relative density of the foam (Gibson and Ashby, 1997). Various hypotheses have been made regarding the 'defect' that diminishes the properties (Simone and Gibson, 1998a,b; Grenestedt and Bassinet, 2000).

1.2. Dynamic mechanical behavior

In order to evaluate the capacity of impact energy absorption, the strain-rate sensitivity of the foam material must be characterized. The Split Hopkinson Pressure Bar (SHPB) method has been widely used in measuring the dynamic compressive response of cellular materials, including polymers and metals.

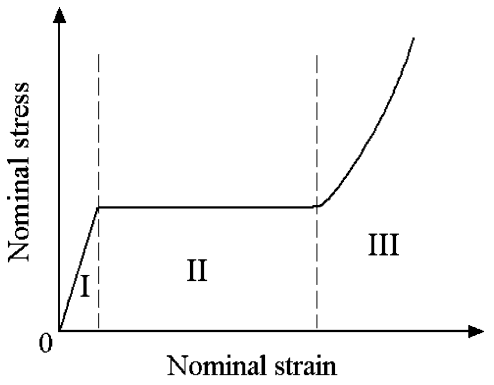

Fig. 1. A typical compressive stress–strain curve of metal foams. Stress–strain curve can be divided into three stages: stage I, the foam deforms linear-elastically; stage II, the foam deforms at almost constant stress and stage III, foam is densified and the stress increases rapidly.

Only limited data are available for the strain-rate dependence of the compression strength of cellular materials. Lankford and Dannemann (1998) reported that the strain-rate dependence was negligible for a low-density open-cell 6101 Al foam. Recently, Deshpande and Fleck (2000) investigated the high strain-rate compressive behavior of a closed-cell aluminum alloy foam Alulight and an open-cell aluminum alloy foam DUOCEL for strain rates up to $5000\ s^{-1}$ using SHPB and direct impact tests. It was found that the dynamic behavior of these foams was very similar to their quasi-static (under strain rate below $10^{-2}\ s^{-1}$) behavior. On the other hand, Mukai et al. (1999a,b) and Kanahashi et al. (2000) reported that an open-cell foam AZ91, an open-cell aluminum foam SG91A and a closed-cell aluminum foam ALPORAS all exhibited high strain-rate sensitivity of the plateau stress. They also found that the absorption energy normalized by the relative density at dynamic strain rates was about 60% higher than that at quasi-static strain rates. Paul and Ramamurty (2000) investigated the strain-rate sensitivity of a closed-cell aluminum foam under nominal strain rates from 3.33×10^{-5} to $1.6\times10^{-1}\ s^{-1}$. Within this range, they found that the plastic strength and the absorbed energy increased by 31% and 52.5%, respectively with the increase in the strain rate. The in-plane dynamic crushing stress of honeycombs was studied both experimentally (Zhao and Gary, 1998) and numerically (Ruan et al., 2003). It was found that increase in the in-plane dynamic crushing stress was not obvious at low impact velocity.

In this paper, an overview is given of the researches on mechanical properties of cellular metals including aluminum honeycombs and foams in the CAS Key Laboratory of Mechanical Behavior and Design of Materials at USTC. The strain-rate effect and micro-structural optimization of cellular metals are reported. Influence of the structural heterogeneity and irregularity on the strain-rate effect of cellular metals is investigated. The effect of

multi-size cell mix and silicate-rubber filler on the mechanical properties of open-cell aluminum foams is studied.

2. Strain-rate effect of cellular metals

In this part, we study the strain-rate effect of cellular metals. Circular-cell aluminum alloy honeycombs are experimentally impacted in the in-plane direction at different velocities. The quasi-static and dynamic behaviors of the circular-cell aluminum alloy honeycombs are investigated. The strain-rate effect and the cell-size effect on the crushing stress of both open-cell and closed-cell aluminum foams are also investigated.

2.1. Dynamic response of aluminum alloy honeycombs

The dynamic behavior of honeycomb is studied using honeycombs with circular holes. The honeycombs are obtained by drilling compact hexagonal-distributed parallel circular holes in an aluminum alloy plate (Chinese brand number LY12). An SHPB apparatus is used to load samples at strain rates of 10^2–$10^3\ s^{-1}$ while an MTS810 testing system is used for quasi-static cases at a strain rate of about $10^{-3}\ s^{-1}$. A comparison of quasi-static and dynamic stress–strain curves of the solid material LY12 does not show any strain-rate sensitivity. The yield strength and the strain-hardening coefficient are about 430 MPa and 2.0 GPa, respectively, while its Young's modulus is about 70 GPa. Two types of cubic honeycomb specimens, $26 \times 25 \times 19\ mm^3$ in dimensions, were prepared and tested (see Table 1 for details). Load is applied in the two in-plane directions: the x_1-direction and the x_2-direction. Fig. 2 shows the geometry of the specimen with

Table 1
Parameters of honeycomb specimens

Type	Cell diameter (mm)	Distance between two adjacent cell centers (mm)	Relative density, ρ^*/ρ_s
1	4.2	5.0	0.36
2	4.0	5.0	0.42

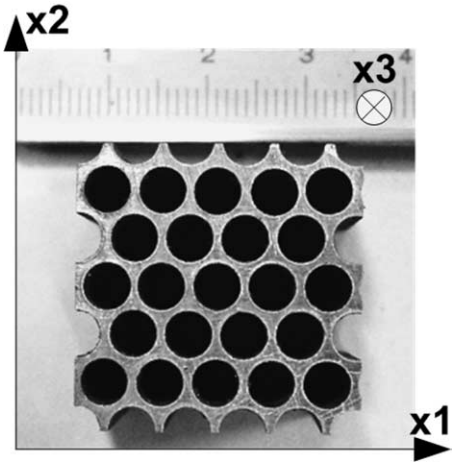

Fig. 2. A honeycomb with hexagonal-distributed circular cells.

cell diameter of 4.2 mm, where ρ^* is the density of honeycombs and ρ_s is the density of the bulk material of honeycombs.

A summary of the experimental results in the x_1-direction compression for two types of circular-cell honeycombs is given in Fig. 3. It transpires that the nominal stress under dynamic compression is higher than that in the quasi-static case. Hence, the mechanical behavior of the honeycombs is sensitive to the impact velocity. However, the nominal stress at an impact velocity of 20 m/s is 15% lower than that at 15 m/s.

To 'freeze' the failure mode, a specimen sleeve is designed to prevent further compression of the specimens. The crushed specimens are compared in Fig. 4. The primary deformation mode of quasi-static compression is shear failure, which propagates from the bottom-left to the top-right (Fig. 4a), and is referred as the shear failure mode. Similar mode is observed in the specimen after impact at 15 m/s (Fig. 4b). At the impact velocity of 20 m/s, shear failure is also observed (Fig. 4c), though its relative compression is low (about 10%). However, due to strong local deformation, a cell wall in the bottom end is broken, as shown by the arrow in Fig. 4b. It transpires that the specimen is easily damaged and fractured under intensely dynamic loading, which is a possible reason for the decrease in the nominal stress when the impact velocity increases from 15 to 20 m/s.

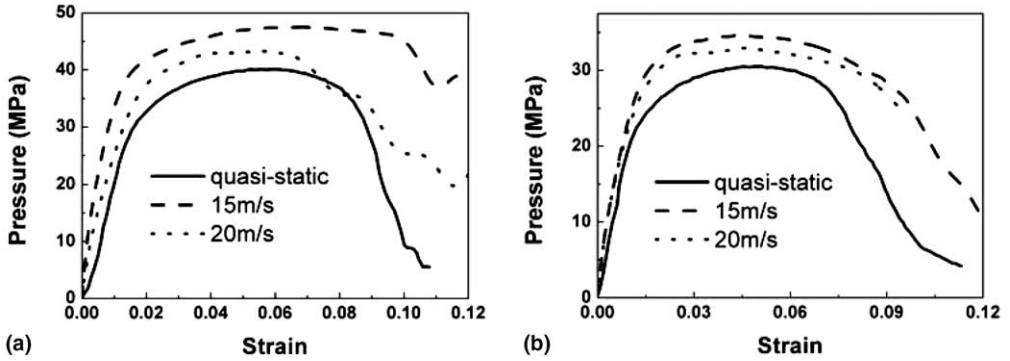

Fig. 3. In-plane crushing behavior of the honeycomb in the x_1-direction: (a) cell diameter of 4.0 mm; (b) cell diameter of 4.2 mm.

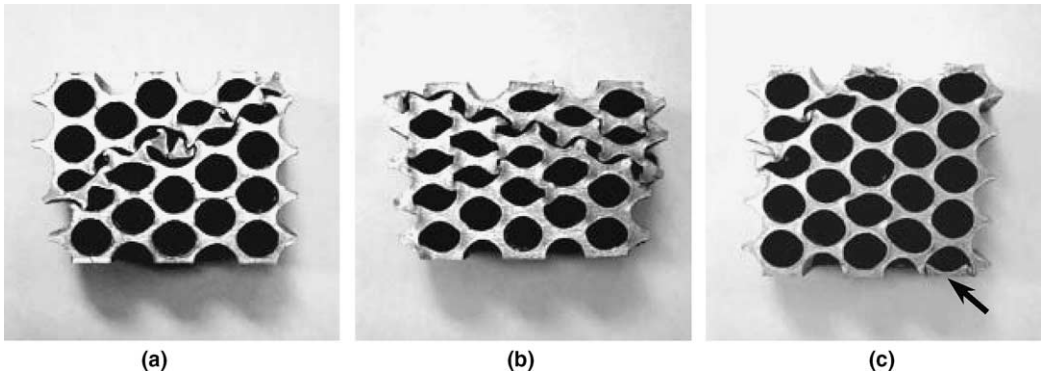

Fig. 4. The frozen crushing modes in the x_1-direction compression: (a) quasi-static; (b) impact velocity of 15 m/s; (c) impact velocity of 20 m/s.

A summary of the experimental results under the x_2-direction compression is presented in Fig. 5. Significant increase in the nominal stress is observed at high loading velocities. For the honeycomb with a cell diameter of 4.0 mm, the nominal stress at an impact velocity of 20 m/s is nearly twice of that at quasi-static compression. For the honeycomb with a cell diameter of 4.2 mm, this increase is nearly 60%. It is found that the behavior of the honeycomb under the x_2-direction compression is very sensitive to the impact velocity. Under dynamic compression, there is an initial nominal stress peak, which is possibly due to the boundary conditions, as the contact area between the specimen and the bars under the x_2-direction compression is much smaller than that under the x_1-direction compression.

Fig. 6 shows photographs of the crushed specimens. The dynamic failure modes at impact velocity of 15 and 20 m/s are very different from those observed in quasi-static cases. It is found that the primary failure mode of quasi-static compression is still the shear failure mode, Fig. 6a. However, under impact loading, the failure mode changes and three types of failure exist: the layer-wise collapse mode (Fig. 6b), the V-shape collapse mode (Fig. 6c and f), and the mixed mode (Fig. 6d and e) including both layer-wise collapse and diagonal shear.

A summary of the maximum nominal stress at different impact velocity is given in Fig. 7. The LY12 aluminum alloy is a strain-rate insensitive material and the in-plane dynamic crushing stress of regular hexagonal honeycombs at low impact

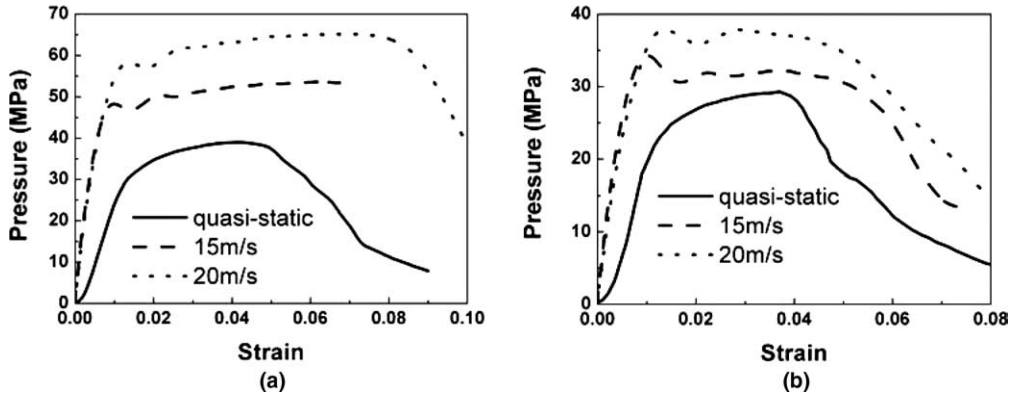

Fig. 5. In-plane crushing behavior of the honeycomb in the x_2-direction: (a) cell diameter of 4.0 mm; (b) cell diameter of 4.2 mm.

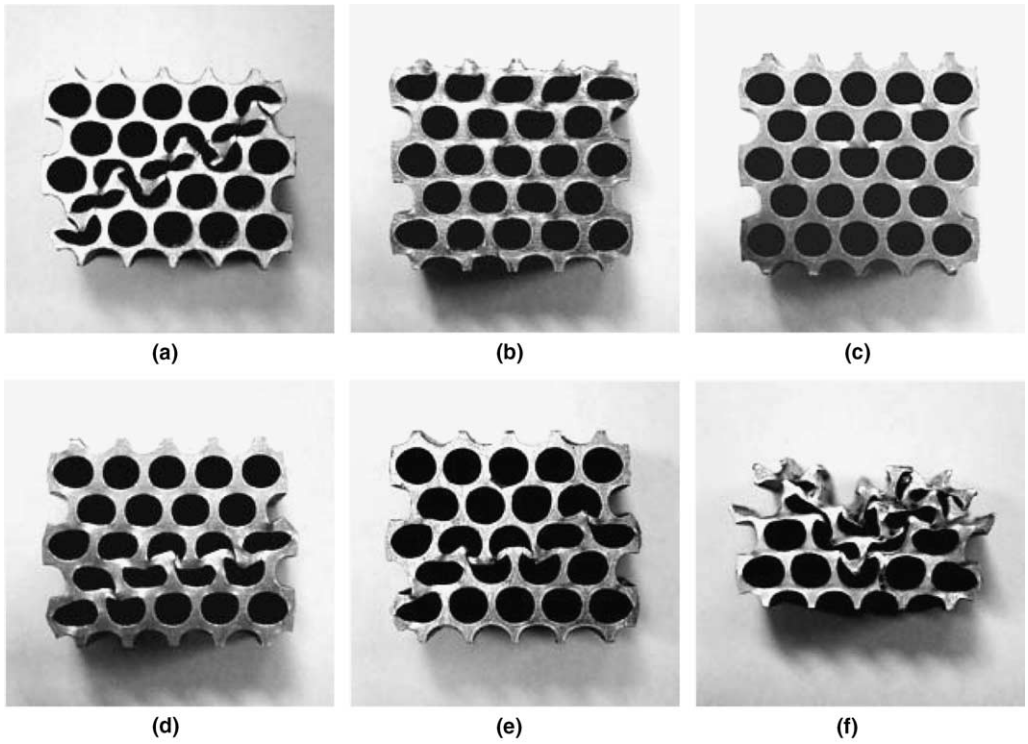

Fig. 6. The frozen crashing modes in the x_2-direction compression: (a) quasi-static; (b)–(d) impact velocity of 15 m/s; (e) and (f) impact velocity of 20 m/s.

velocities is insensitive to the impact velocity (Zhao and Gary, 1998; Ruan et al., 2003). It can be inferred that the strain-rate sensitivity of the honeycomb specimens to the loading velocity is attributed to the structural or the local inertia effect caused by structural heterogeneity, for there are obvious plateau zone between the adjacent cells in the circular-cell honeycombs. It is interesting to note that the maximum nominal stresses in the x_1- and x_2-directions are almost the same

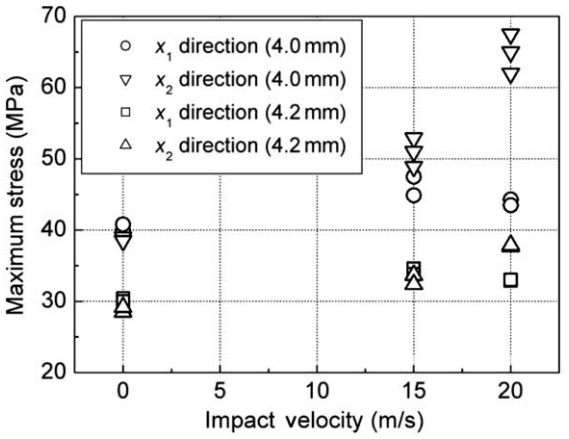

Fig. 7. The maximum nominal stress at different impact velocities.

before the impact velocity reaches 15 m/s. From Fig. 7, we can see that the maximal nominal stress changes dramatically when the impact velocity reaches 20 m/s.

2.2. Strain-rate effect and cell-size effect of metallic foams

The quasi-static and dynamic compressive behaviors of two kinds of aluminum foams are examined. Open-cell aluminum foams and closed-cell aluminum alloy foams were produced by infiltration method and powder metallurgical method, respectively. Cylindrical specimens are used. The size is $\varnothing$ 35 mm × 10 mm and $\varnothing$ 30 mm × 25 mm for dynamic and quasi-static tests, respectively. Again, MTS810 and SHPB testing systems are used.

Fig. 8 shows the experimental results of the closed-cell aluminum alloy foams with a relative density of 0.23 but different in average cell size. It is evident that cell size has significant effect on the plateau stress of the closed-cell foams. The responses of the foams with different average cell sizes are different, meanwhile the effect in dynamic cases are more significant than that in quasi-static case.

Fig. 9 shows the experimental results of the engineering quasi-static and dynamic compressive stress–strain curves of the open-cell aluminum foams with a relative density of 40% and different cell sizes. Both the size effect and strain-rate effect are obvious.

3. Micro-structural optimization of open-cell aluminum foams

In this part, we study micro-structural optimization for open-cell aluminum foams. Open-cell aluminum foams with multi-size cell distribution are manufactured. The effect of multi-size cell mix on the mechanical properties of open-cell aluminum foams is studied by experiments and

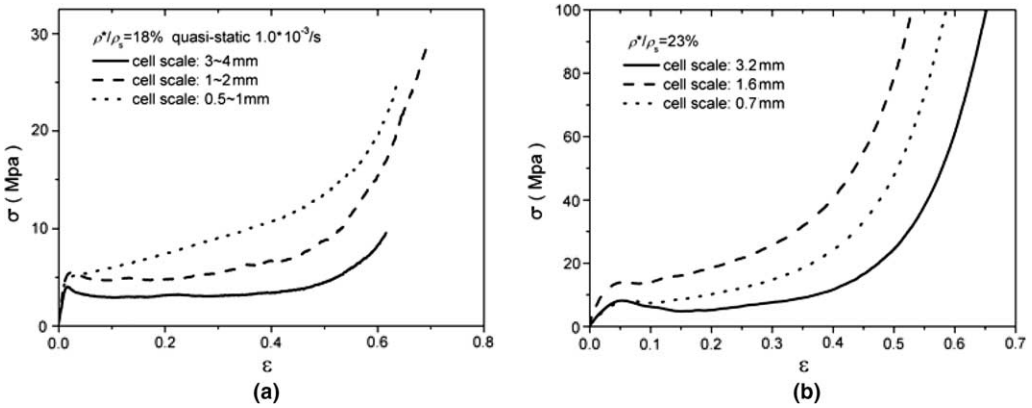

Fig. 8. Compressive stress–strain curves of closed-cell aluminum foams with identical density but different cell size under (a) quasi-static loading and (b) dynamic loading.

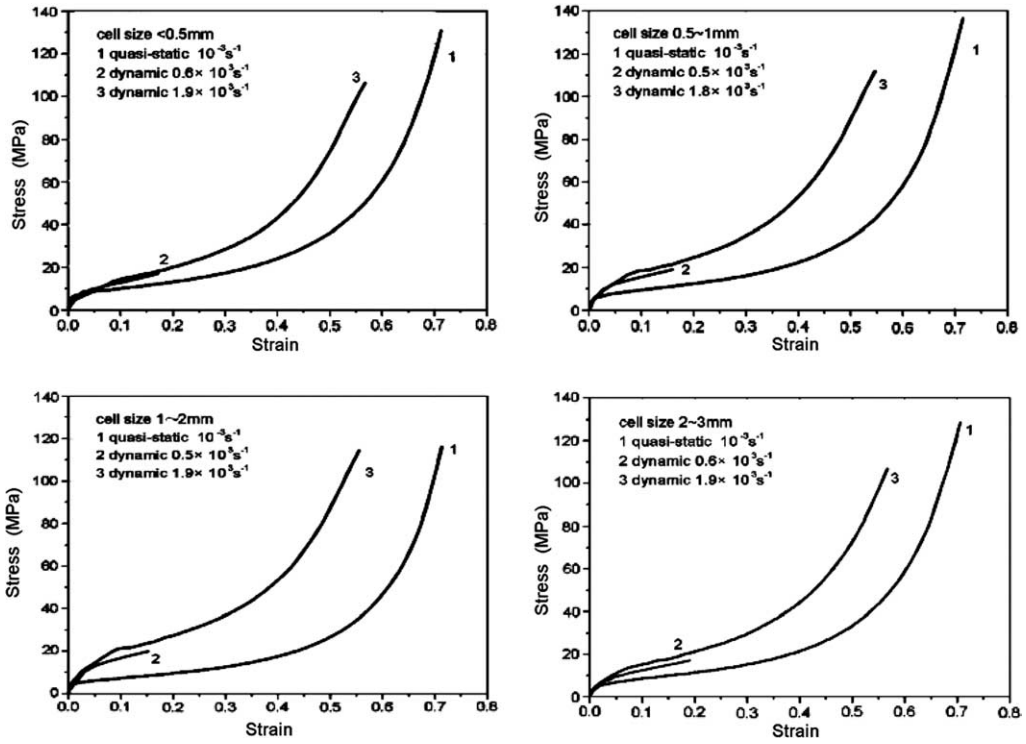

Fig. 9. The engineering quasi-static and dynamic compressive stress–strain curves of open-cell aluminum foams with relative density of 40% and different cell size.

numerical simulations (for details, see Li et al., 2003). Silicate-rubber is filled into open-cell aluminum foams to improve their mechanical behaviors. The influence of filler fraction and constraint conditions on the mechanical properties of open-cell aluminum foams are investigated.

3.1. Effect of dual-size mix on the mechanical properties of open-cell aluminum foams

Open-cell aluminum foams with dual-size cells are produced by infiltration method. Fig. 10 shows the microstructures of the aluminum foam materials with different small cell fraction. The volume-fraction ratio of small-size cells (~0.5 mm) to large-size cells (~2.5 mm), η, in Fig. 10a, is 0.25, while that in Fig. 10b is 0.67. In foams with multi-size cells, the small cells are normally congregated in the corner between large-size cells, i.e., occupy the nodal zone or the plateau zone, as shown in Fig. 10a. A comparison of typical compressive stress–strain curves of foams with uniform cell size and dual cell size is given in Fig. 11. It transpires that the cellular material with mixed cell size has a much higher stiffness (about 650 MPa) than that with uniform cell size (260 MPa) even the relative density of the former is a little lower. On the other hand, the strength of the two foam materials shows little difference. However, when η increases, more small cells occupy the middle spans, Fig. 10b. This will reduce the stiffness. Our experiments have shown that the stiffness of foam is less than that with $\eta = 0.2$ when their relative density is the same.

Here, we use two-dimensional finite element analysis to explore the influence and mechanism of cell mix on the elastic modulus and plateau strength of open-cell aluminum foams, and ABAQUS/Standard V5.8 code is used for finite element analyses. For simplicity, ideal honeycomb model materials as a two-dimensional counterpart of the three-dimensional foams are used. Though

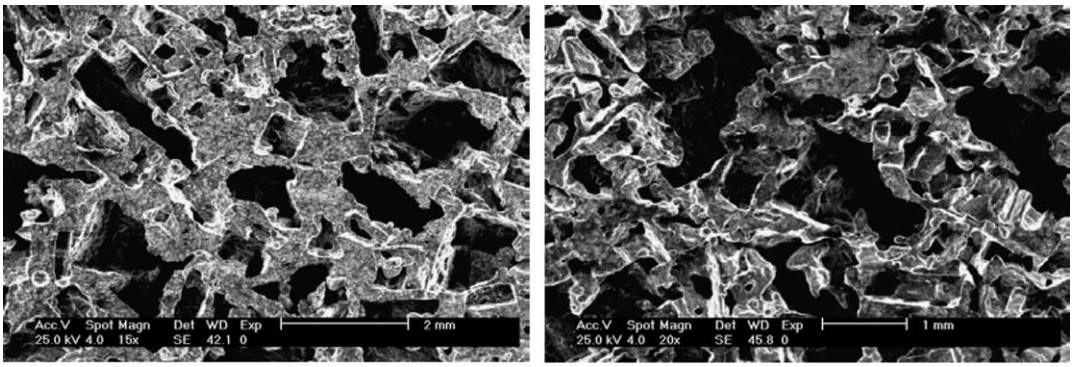

Fig. 10. SEM photos of open-cell aluminum foams with dual-size mix, the volume ratio of small cells to big cells is (a) 0.25 and (b) 0.67.

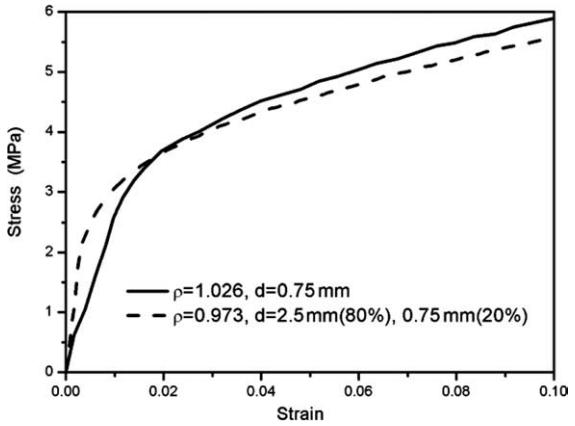

Fig. 11. A comparison of mechanical behavior between foams with uniform cell size and dual cell size.

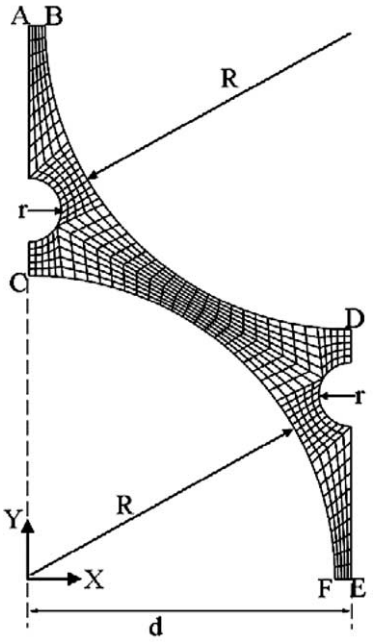

Fig. 12. Sample finite element mesh for the unit cell used in calculation, $r = 0.1d$, and $R = 0.94d$.

the cell shape is irregular in practice, a circular shape is assumed to ignore the cell shape effect and keep the configuration of the plateau border. Different small-cell sizes and thus different relative densities, ρ^*/ρ_s, are used to investigate the effects of the dual-size-cell structure. Fig. 12 shows the representative cell model used in the finite element analyses. Isotropic material model with elastic-perfectly plastic stress–strain behavior is assumed to eliminate any dependence of the results on a chosen strain-hardening exponent. Parameters used in the isotropic elastic-perfectly plastic model are $E_s = 70$ GPa, $v = 0.33$ and $\sigma_{ys} = 150$ MPa.

Compressive load is applied in the y-direction. Assuming small cells and large cells are mixed together, the radius of the large cells is R, and the distance of two adjacent large cells is $2d$. In the representative volume element, the symmetric boundary condition in the x-direction is applied to line AC, the symmetric boundary condition in the y-direction is applied to line FE. The periodic boundary condition in the x-direction is applied

to line DE, and the displacement boundary condition in the y-direction is applied to line AB. The reaction forces on the nodes of the displaced boundary are recorded and summed in order to compute the overall stress at each increment of displacement. The stress of 2% strain or the maximum stress (if the maximum stress is reached before the strain of 2%) is chosen as the yield strength.

In our numerical simulation, we consider four values of r, i.e., $r = 0.10d$, $r = 0.15d$, $r = 0.20d$, and $r = 0$ which corresponds to single-size cells. Different sizes of the large cells are used, given a relative density ranging from about 0.19 to 0.42. In all these cases, the small cells are assumed located regularly.

Fig. 13a and b shows the dependence of the relative modulus E^*/E_s and the relative strength σ^*/σ_{ys} to the relative density of the honeycomb for different small-cell sizes, respectively. The numerical results indicate that both the stiffness and the yield strength increase if small cells with low volume fraction are added. With small cells $0.20d$ in radius, the honeycomb shows the largest increase in stiffness; while with small cells $0.10d$ or $0.15d$ in radius, the honeycomb shows the largest increase in yield strength. This suggests that both the stiffness and the strength can be increased if small cells with proper size and volume fraction are added.

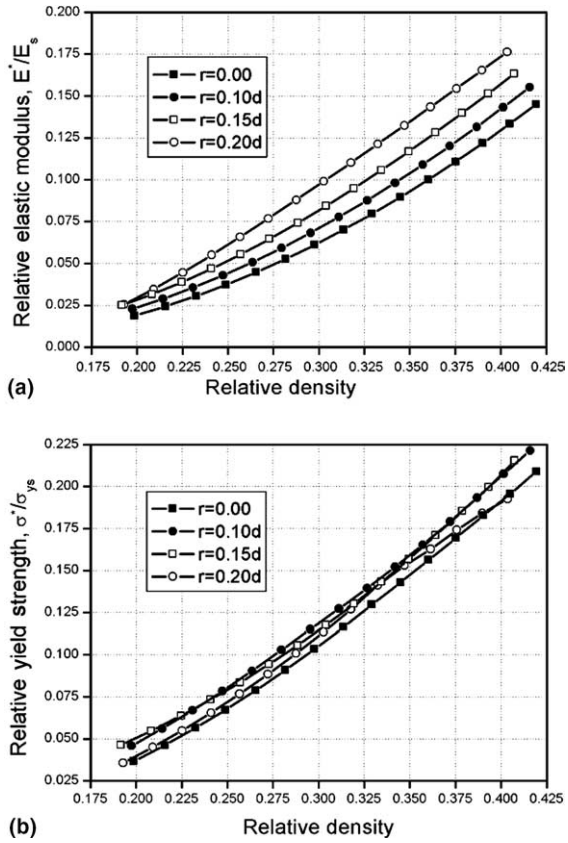

Fig. 13. FEA results of mechanical behavior of honeycomb with mixed cells: (a) relative modulus vs. relative density and (b) relative strength vs. relative density.

3.2. Mechanical behavior of open-cell aluminum foams with silicate-rubber filler

Aluminum foams are often used for impact energy absorption, whilst rubbers are effective impact-protection materials and have long been used as cushions, vibration reducers and impact energy absorbers. Therefore, a combination of rubber with open-cell aluminum foams may provide a new composite with improved mechanical property and energy absorption capacity.

The open-cell aluminum foams used in our investigation were made of commercially pure aluminum and produced by the infiltration method. The average cell size is 2 mm and the relative density is about 0.43. Silicate-rubber was infiltrated into the open-cell foam. Fig. 14 shows the struc-

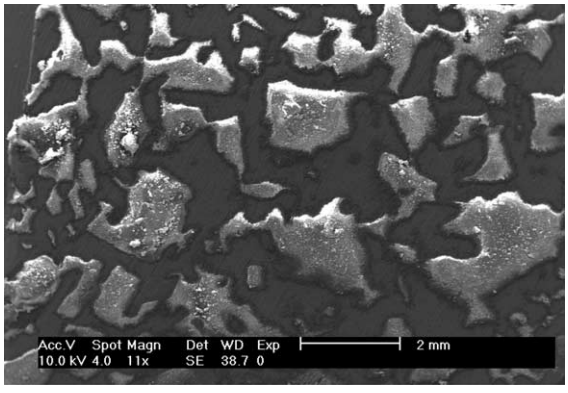

Fig. 14. SEM image of an open-cell aluminum foam with silicate-rubber filler.

ture of the open-cell aluminum foams with silicate-rubber filler.

A comparison of the uniaxial compressive stress–strain curves of the open-cell aluminum foams with or without silicate-rubber filler is shown in Fig. 15. It is obvious that after filling with the silicate-rubber, the compressive stress–strain curve exhibits a prolonged plateau region without distinct densification, indicating a better energy absorption capacity.

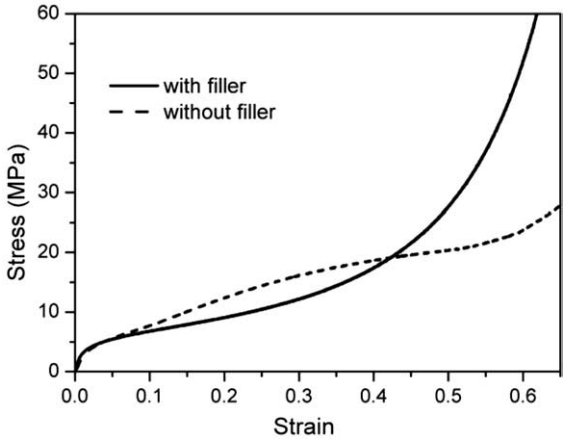

Fig. 15. Uniaxial compressive stress–strain curves of open-cell aluminum foams with or without filler.

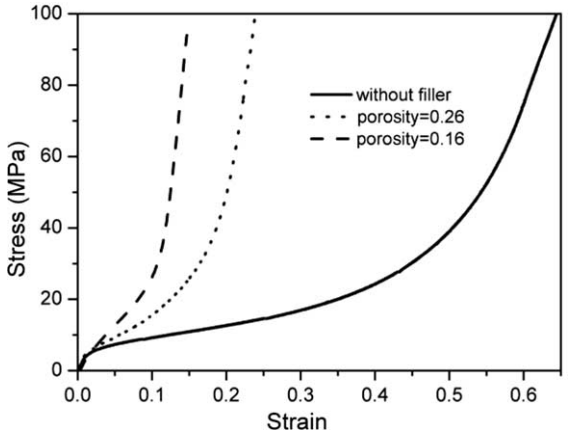

Fig. 16. Lateral-constrained compressive stress–strain curves of open-cell aluminum foams with silicate-rubber filler of different volume fraction.

On the other hand, the foam/rubber composite exhibits a similar response to the constrained loading. Fig. 16 shows the lateral-constrained compressive stress–strain curves of the open-cell aluminum foams with silicate-rubber filler of different volume fraction. Different bulk compressive properties of the open-cell aluminum foams can be obtained by changing the volume fraction of the silicate-rubber. Therefore, this composite shows a potential to control its response by change of the constraint condition or volume fraction of the filling rubber.

4. Concluding remarks

The strain-rate effect and micro-structural optimization of cellular metals are investigated. The in-plane quasi-static and dynamic behavior of circular-cell aluminum alloy honeycombs shows that impact velocity has significant influence on the localized deformation mode and the plateau stress, which means that the structural heterogeneity induce the strain-rate effect of circular-cell honeycombs. The strain-rate effect and the cell-size effect on the crushing stress of both open-cell and closed-cell aluminum foams are found. The effect of multi-size cell mix and silicate-rubber filler on the mechanical properties of open-cell aluminum foams is studied. Results show that the mechanical properties of open-cell foams can be further improved by mixing small cells with proper size and volume fraction during manufacture or by further infiltrating some ultra-light, ductile material such as silicate-rubber.

Acknowledgments

This work reported herein is supported by the National Natural Science Foundation of China (Projects No. 10072059, No. 90205003 and No. 10302027) and the CAS K.C. Wong Post-doctoral Research Award Fund. The authors wish to thank Dr. Hefa Cheng, Mr. Yi Pan and Mr. Erheng Wang for their assistance and useful discussions.

References

Andrews, E., Sanders, W., Gibson, L.J., 1999. Compressive and tensile behaviour of aluminum foams. Mater. Sci. Engng. A 270, 113–124.

Beals, J.T., Thompson, M.S., 1997. Density gradient effects on aluminium foam compression behaviour. J. Mater. Sci. 32, 3595–3600.

Deshpande, V.S., Fleck, N.A., 2000. High strain rate compressive behaviour of aluminium alloy foams. Int. J. Impact Engng. 24, 277–298.

Gibson, L.J., Ashby, M.F., 1997. Cellular Solids: Structure and Properties. Pergamon, Oxford.

Grenestedt, J.L., Bassinet, F., 2000. Influence of cell wall thickness variations on elastic stiffness of closed-cell cellular solids. Int. J. Mech. Sci. 42, 1327–1338.

Kanahashi, H., Mukai, T., Yamada, Y., Shimojima, K., Mabuchi, M., Nieh, T.G., Higashi, K., 2000. Dynamic compression of an ultra-low density aluminium foam. Mater. Sci. Engng. A 280 (2), 349–353.

Lankford, J., Dannemann, K.A., 1998. Strain rate effects in porous materialsSymposium Proceedings 521, Porous and Cellular Materials for Structure Applications. Materials Research Society, Warrendale, pp. 103–108.

Li, J.R., Cheng, H.F., Yu, J.L., Han, F.S., 2003. Effect of dual-size cell mix on the stiffness and strength of open-cell aluminum foams. Mater. Sci. Engng. A 362, 240–248.

Mukai, T., Kanahashi, H., Miyoshi, T., Mabuchi, M., Nieh, T.G., Higashi, K., 1999a. Experimental study of energy absorption in a close-celled aluminum foam under dynamic loading. Scr. Mater. 40 (8), 921–927.

Mukai, T., Kanahashi, H., Yamada, Y., Shimojima, K., Mabuchi, M., Nieh, T.G., Higashi, K., 1999b. Dynamic compressive behavior of an ultra-lightweight magnesium foam. Scr. Mater. 41 (4), 365–371.

Paul, A., Ramamurty, U., 2000. Strain rate sensitivity of a closed aluminum foam. Mater. Sci. Engng. A 281 (1), 1–7.

Prakash, O., Sang, H., Embury, J.D., 1995. Structure and properties of Al–SiC foam. Mater. Sci. Engng. A 199, 195–203.

Ruan, D., Lu, G., Wang, B., Yu, T.X., 2003. In-plane dynamic crushing of honeycombs—a finite element study. Int. J. Impact Engng. 28, 161–182.

Simone, A.E., Gibson, L.J., 1998a. Effects of solid distribution on the stiffness and strength of metallic foams. Acta Mater. 46 (6), 2139–2150.

Simone, A.E., Gibson, L.J., 1998b. The effects of cell face curvature and corrugations on the stiffness and strength of metallic foams. Acta Mater. 46 (11), 3929–3935.

Sugimura, Y., Meyer, J., He, M.Y., Bart-Smith, H., Grenstedt, J.L., Evans, A.G., 1997. On the mechanical performance of closed cell Al alloy foams. Acta Mater. 45 (12), 5245–5259.

Zhao, H., Gary, G., 1998. Crushing behaviour of aluminium honeycombs under impact loading. Int. J. Impact Engng. 21, 827–836.